Available online at www.sciencedirect.com
SCIENCE DIRECT®
Journal of Colloid and Interface Science 264 (2003) 195–202
JOURNAL OF Colloid and Interface Science
www.elsevier.com/locate/jcis

On the behavior of electrokinetic streaming potential during protein filtration with fully and partially retentive nanopores

Jun Hee Sung,[a] Myung-Suk Chun,[b,*] and Hyoung Jin Choi [a]

[a] *Department of Polymer Science and Engineering, Inha University, Incheon 402-751, South Korea*
[b] *Complex Fluids and Membrane Team, Korea Institute of Science and Technology (KIST), P.O. Box 131, Cheongryang, Seoul 130-650, South Korea*

Received 6 December 2002; accepted 26 March 2003

Abstract

An experimental investigation of the electrokinetic streaming potentials of both fully and partially retentive nanopores as compared with the filtration progress of dilute globular protein solution under different surface charge conditions was performed using hollow fibers. The streaming potential is generated by the electrokinetic flow effect within the electric double layer of the charged surface. Depending on the solution pH, both the protein and the pore wall can be either repulsive or attractive due to the long-range electrostatic interaction. The repulsive electrostatic interaction allows the protein particles to stay in a suspended state above the outer surface of hollow fibers instead of being deposited. The apparent streaming potential value at partially retentive pores is larger than that at fully retentive pores for the oppositely charged case; however, the opposite behavior is shown for the same-charged case. The axial-position-dependent streaming potential was also observed in order to explore the development of a concentration polarization layer during the cross-flow filtration. The time evolution of the streaming potential during the filtration of protein particles is related to the filtrate flux, from which it can be found to provide useful real-time information on particle deposition onto the outer surfaces of hollow fibers.

Keywords: Streaming potential; Electrokinetic flow; Nanopore; Bovine serum albumin; Electrostatic interaction; Hollow fibers; Filtration flux

1. Introduction

There has been considerable interest in the characterization of surface properties of filtration membranes. These properties have been shown to influence filtrate flux, membrane fouling, and solute rejection. Different methods based on electrokinetic phenomena have been used to determine the electric properties of membranes. Among them, measuring the flow-induced streaming potential became the most widely used technique, because it can be easily used to characterize the electric properties of both the pore surfaces and the outer surface of the membrane [1–10].

Three kinds of situations can be considered in the experiments with filtration membranes, where the pore size has a nanometer order. The first one is that the fluid flows through the pore, and there is no particle deposition onto the membrane surface [4,7]. Once the particle suspension flows through the pore, there exist two cases, full retention and partial retention, according to the pore size compared to the particle size. Full retention becomes partial retention when the pore size is larger than the particle size. In the case of partially retentive filtration, the interaction between the particle and the pore wall should be considered [5,9,10]. Whatever situations are undertaken, the evolution of the streaming potential behavior during the filtration of particles is important. Both the cake layer and the concentration polarization layer developed on the outer surface of the membrane influence upon the streaming potential, which suggests the possible application of the streaming potential to a monitoring the fouling.

Due to the electrostatic interaction, the streaming potential behavior can be changed by the surface charge conditions of both the pore wall and the particles. The electrostatic repulsion exists between the pore wall and the particles for the same (i.e., like) charged case, whereas electrostatic attraction is involved for the oppositely charged case. The surface charge conditions are determined by the solution pH, which means that the surface is positively charged or negatively charged around the isoelectric point.

* Corresponding author.
E-mail address: mschun@kist.re.kr (M.-S. Chun).

0021-9797/03/$ – see front matter
doi:10.1016/S0021-9797(03)00352-7

In this work, an explicit comparison of streaming potential behavior between the fully retentive and the partially retentive nanopores with the time progress of hollow-fiber filtration is investigated. A dilute suspension of bovine serum albumin (BSA) protein was prepared and commercially available hollow fibers were chosen. The streaming potentials are examined for solutions at pH 6.0 as well as 10.0, since the pH changes the surface charge conditions of both the protein particle and the pore wall. The axial-position-dependent streaming potential was also observed in order to identify the effect of the concentration polarization layer generated during the cross-flow filtration. We point out that most studies on the streaming potential measurements have been devoted to flat-plate or tubular membranes, so far. Unlike these types, a hollow-fiber membrane is not advantageous in that it has a very narrow internal diameter, and this fact results in really difficulty in installing internal electrodes and also becomes liable to damage the hollow fiber. In this respect, a challenge to streaming potential measurements for nanopores of hollow fiber reasonably rises to a significance guaranteeing the technique.

2. Flow-induced streaming potential principle

The electric double layer (EDL) that is formed at the phase boundary between a solid and a liquid determines the electrokinetic properties of solid materials. Several mechanisms such as dissociation of surface functional groups, adsorption of ions, and adsorption of charged molecules account for the surface charges of polymeric membranes contacted with aqueous solutions. In an electric field governed by the Poisson–Boltzmann (P–B) equation, the thickness of the EDL at the phase boundary can be quantified by the Debye length. The inverse Debye length κ is defined by

$$\kappa = \left[\frac{2n_{i,b}Z_i^2e^2}{\varepsilon kT}\right]^{1/2}, \tag{1}$$

where $n_{i,b}$ is the concentration of the type i ion in the bulk solution, Z_i the valence of the type i ion, e the elementary charge, ε the dielectric constant, and kT the Boltzmann thermal energy. For a dimensionless low potential of $\Psi \leqslant 1$ (i.e., less than $kT/e = 25.69$ mV) with a 1:1 electrolyte system, the P–B equation may be linearized, which is called the Debye–Hückel equation [11].

When the electrolyte solution is forced to flow through a solid channel by means of external pressure, an electric potential difference or streaming potential between the two ends of the channel can be measured. The ions are stripped off along the shear plane due to the pressure P, and a streaming current is formed. Charge accumulation at the downstream side generates an electric field that causes a backflow of ions until a steady state is reached. The electrokinetic streaming potential E gives direct information about the electrostatic charge at the EDL shear plane [12,13].

The fundamental relationship between the measured streaming potential E and the zeta potential ζ is given by the well-known Helmholtz–Smoluchowski (H–S) equation [14],

$$\frac{\Delta E}{\Delta P} = \frac{\varepsilon\zeta}{\eta\lambda_0}, \tag{2}$$

where η is the solution viscosity and λ_0 the solution conductivity. The linear relationship between ΔE and ΔP can be obtained from the streaming potential difference ΔE measured with variations of the trans-pore pressure drop ΔP. Equation (2) is reasonably applied to surfaces with low surface conduction compared to the solution conduction. The zeta potential, defined as the potential at the shear plane between the Stern layer and the mobile diffuse layer, is commonly used as the electrokinetic value.

It should be noted that, when the EDL thickness exceeds the pore radius, a rigorous interpretation in terms of the H–S formula is inevitably limited. The overlap of EDL inside the pore results in a concentration gradient across the pore, and subsequently the solution conductivity at the pore region will deviate from its bulk value. The membrane potential caused by this concentration gradient is added to the pressure-induced streaming potential, on which the filtration potential has been acknowledged very recently [15]. The streaming potential defined in this study means the apparent one, which allows us favorably to examine its behavior or trends in the hollow fiber without complicated calculations.

3. Experiments

3.1. Model globular protein and hollow fiber

Bovine serum albumin (BSA), used as a model protein, was purchased from Sigma Chemical Co. (St. Louis, MO). This was prepared from fraction V (A-3059) and then crystallized and lyophilized. The BSA particle has been evaluated as a prolate ellipsoid of $14.1 \times 4.1 \times 4.1$ nm with average molecular weight 6.9×10^4 Da. The equivalent hydrodynamic radius of the BSA particle is known to be 3.2 nm, which is taken as the particle radius plus the distance to the outer Helmholtz plane as the particle moves through the electrolyte solution [16]. The zeta potential of BSA protein, determined using a Zeta-Plus (Brookhaven Instrument Co., NY) was calculated from the mobility values based on a Doppler principle together with the particle velocity obtained by Smoluchowski formula. Filtration experiments were carried out using 90 ppm BSA suspensions with 1.0 mM KCl electrolyte. The pH was adjusted by the addition of 0.05 M HCl and 0.05 M NaOH aqueous solutions.

We used the commercially available hydrophobic polysulfone PM10 and PM100 (Koch Membrane System Inc., MA) hollow fibers, with inner and outer diameters of 0.11 and 0.21 cm. The molecular weight cut-offs correspond to 10 and 100 kDa, and the mean diameters of the pore in the skin layer are estimated as 3.1 and 11.0 nm, respectively [10].

The hollow fibers were rinsed with distilled water to remove the wetting agent prior to use. The rejection for the BSA suspension was determined by a comparison of BSA concentrations in the feed and in the filtrate using a refractive index detector (RI 2000, Schambeck SFD GmbH, Germany). The rejection of the PM10 hollow fiber shows 98.5% for pH 6 and 99% for pH 10, indicating fully retentive behavior. The PM100 results in 35 and 37% rejections for pH 6 and 10, respectively, reflecting partially retentive behavior.

3.2. Surface composition and morphological characterization of hollow fiber

Surface chemical characterization was carried out by X-ray photoelectron spectroscopy (XPS) using a Physical Electronics PHI 5800 spectrometer with non-monochromatic Al Kα radiation (350 W, 15 kV, 1253.6 eV) as excitation source. High-resolution spectra were recorded at a take-off angle of 45° by a concentric hemispherical analyzer operating in constant pass energy mode (at 187.85 and 23.5 eV for wide scan and narrow scan, respectively), using a 400-μm-diameter analysis area. Hollow fibers were irradiated for a maximum time of 15 min to minimize X-ray induced sample damage. Atomic concentration percentages were determined from the different measured spectral regions by taking into account the corresponding area sensitivity factor.

Atomic force microscopy (AFM) imaging allows expecting a comparison of the surfaces of the virgin hollow fiber before the BSA filtration and the fouled one after the BSA filtration. The AFM used was an Autoprobe CP (Park Scientific Instruments, CA) in double-layer mode with a scan rate of 1 Hz at 256 × 256 resolution in 1.0 mM KCl solution. The cantilevers used were Si_3N_4 microlevers with a specified spring constant of 0.563 N/m. For surface images and line profiles the AFM imaging software was employed.

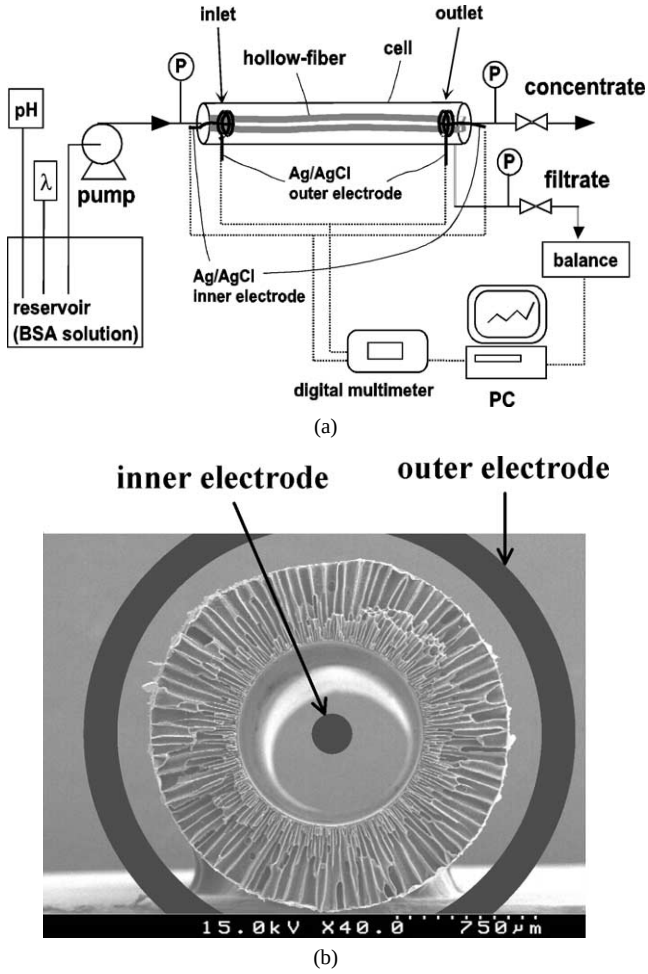

Fig. 1. (a) Experimental setup for in situ measurements of both local streaming potential and filtrate flux. (b) Scanning image of field emission scanning electron microscopy (FE-SEM, Hitachi, S-4200) for cross-sectional view of PM10 hollow fiber and a schematic of the locations of the inner and outer electrodes.

3.3. Streaming potential and filtrate flux measurements

Except for the streaming potential cell equipped with a single hollow fiber, detailed descriptions of the system shown in Fig. 1a are similar to those in previous studies (e.g., [2,4,9,10]). The streaming potential cell has dimensions 0.31 cm in inner diameter and 12 cm in effective length, wherein the ends of the cell were potted with cured epoxy resin in order to place a hollow fiber. For the streaming potential differences at inlet as well as outlet positions of a hollow fiber, pairs of Ag/AgCl electrodes were installed very carefully both inside and outside each position as schematically illustrated in Fig. 1b. The Ag/AgCl electrodes were prepared by anodic deposition of chloride on silver with a DC power supply (Consort E832, Belgium) at 0.4 mA/cm^2 for 30 min. A wire-type electrode 0.25 mm in diameter installed inside the hollow fiber takes about 6% of the internal cross-sectional area of the hollow fiber to allow an undisturbed flow condition. A spiral electrode is suitably installed on the corresponding external positions of the hollow fiber so that it can detect the minute streaming potential difference.

After the system was stabilized at a given ΔP, the streaming potential difference between the inside and outside of the hollow fiber was measured using a digital multimeter (HP34970A, Hewlett-Packard Co., CA) connected to the two pairs of electrodes at both inlet and outlet positions. Pressure was supplied by a high-precision metering pump (M920, YoungLin Co., Seoul) and measured by a transducer and a digital readout. Trans-pore pressure was adjusted up to 0.3% of the maximum flow rate using a micrometer capillary valve (Gilmont Inst., IL). The streaming potential difference was measured with variations of the trans-pore pressure drop, for which several discrete pressures (i.e., 4 or 5) around 2.5 bar were generated, with the system allowed to equilibrate at each pressure. Solution conductivity, λ_0, was measured using a conductivity meter (Model 32, YSI, OH).

The amount of BSA filtrate collected over time was determined by continuously weighing it on an electric balance (Mettler, Model PG502, Switzerland), and then it was registered by data acquisition program (BalanceLink Version 2.20, Mettler-Toledo AG). The effect of the solution pH upon both the streaming potential and the filtration flux has been examined with simultaneous monitoring of time progress. We also measured the axial-position-dependent streaming potential of the pore due to the origin of the cross-flow through the inner channel of hollow fiber.

4. Results and discussion

4.1. Surface charge characterization

Relative percentages of atomic concentrations for the polysulfone characteristic elements (C, O, S) are given in Table 1. The existence of N was obtained, and it can be seen a difference between relative percentages for the outside of the skin layer and that of the support layer. The values of C and O obtained for PM10 differ somewhat from the values either obtained for UDEL polysulfone (Union Carbide, CT) or reported in the literature [17].

We found that measurements of streaming potential were highly reproducible, confirming the precision. For the range from 0.1 to 0.4 bar, a linear relationship between ΔE and ΔP can be seen in Fig. 2. Applying Eq. (2) determines the apparent zeta potential of the hollow fiber related to the electrokinetic properties of the pore, where the variability of the zeta potential values is less than 8%. The concentration gradient across the pore results in an initial nonlinearity observed in ΔP of less than 0.1 bar. This initial nonlinearity was also caused by a shift in the zero-pressure intercept as shown in pH 10.0 and 11.1 due to small asymmetries in the electrodes. The conductivity of the bulk solution λ_0 shows a minimum value of $1.32 \times 10^{-2}\ \Omega^{-1}$ m at pH 7.0, while it is increased with either pH decreasing or pH increasing, to $3.42 \times 10^{-2}\ \Omega^{-1}$ m at pH 3.0 and $1.96 \times 10^{-2}\ \Omega^{-1}$ m at pH 10.0.

Table 1
Surface atomic concentrations determined by XPS experiments

Sample	C (%)	N (%)	O (%)	S (%)
PM10				
(outside of skin layer)	75.0	1.7	21.1	2.2
(outside of support layer)	79.9	2.4	15.3	2.4
UDEL	84.8	1.1	11.6	2.5

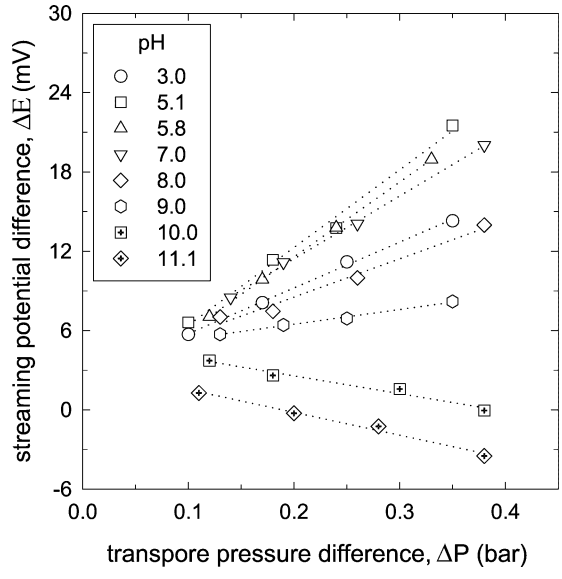

Fig. 2. The apparent streaming potential (ΔE) versus transpore pressure difference (ΔP) with different pH at 1.0 mM KCl electrolyte solution for PM100.

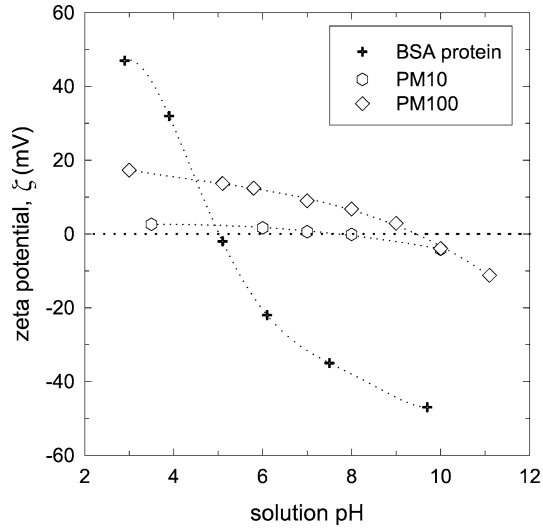

Fig. 3. The zeta potential characterization of BSA protein and model hollow fibers; zeta potential for hollow fibers represents the apparent one.

Figure 3 shows that the zeta potentials of both the pore surfaces and the BSA change from positive to negative with the increase of solution pH. The isoelectric points of pore surfaces for PM10 and PM100 are formed around pH 7.4 and 9.3, respectively. As observed in the literature [18], decreasing pore size gives a shift of the isoelectric point to lower pH values due to a difference in the number of charges. The isoelectric point of BSA appears around pH 4.9, which agrees with the value widely reported in the literature [19]. The variance range of the zeta potential of BSA particle is larger than that of the pore surfaces; therefore, both PM10 and PM100 are considered to be weakly charged compared to BSA.

4.2. Comparisons between fully retentive and partially retentive pores

Two series of results for full and partial retention were obtained with PM10 and PM100, respectively. The variations of the streaming potential coefficient ($= \Delta E/\Delta P$) as the time progresses were observed for the solutions of pH 6.0 and 10.0. The ionic concentration of 1.0 mM of KCl elec-

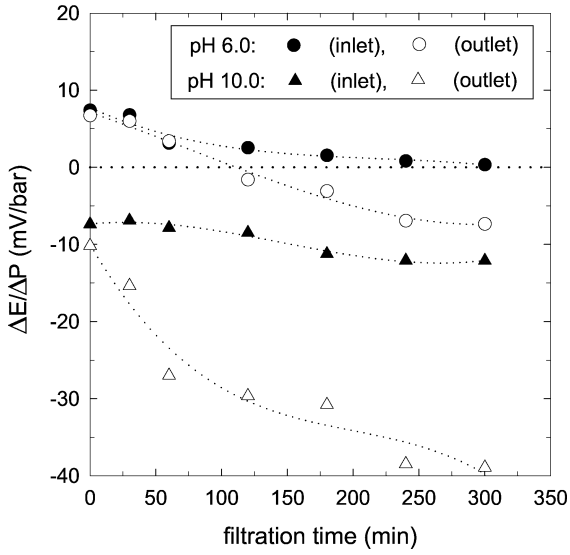

Fig. 4. Changes in the streaming potential of a fully retentive pore (PM10) during the filtration of 90 ppm BSA solution for same-charged (pH 10.0) and oppositely charged (pH 6.0) cases, with 1.0 mM KCl concentration.

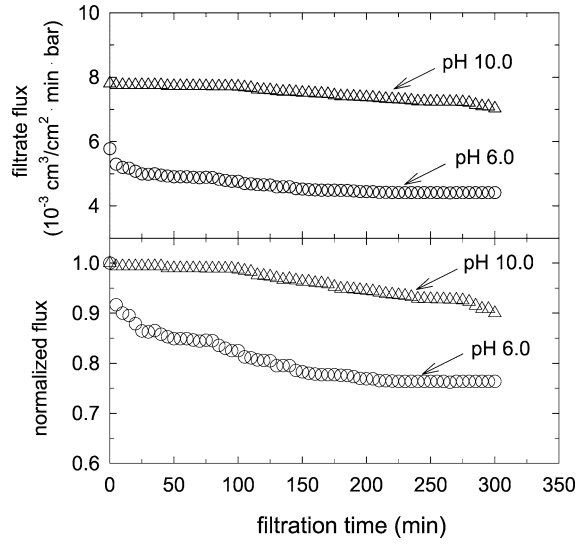

Fig. 5. Changes in the filtrate flux of fully retentive pore (PM10) during the filtration of 90 ppm BSA solution for same-charged (pH 10.0) and oppositely charged (pH 6.0) cases, with 1.0 mM KCl concentration.

trolyte at 25 °C corresponds to the Debye length of 9.7 nm using Eq. (1), which is larger than the mean pore radius. We consider here the time evolution behavior instead of the rigorous estimation of the zeta potential. A variation of solution pH leads to a displacement of the surface acid–base equilibrium, and subsequently the net charge of the surface is modified, as provided in Fig. 3. While the surfaces of the BSA particle and the pore wall become oppositely charged at pH 6.0, they employ a same-charged condition with negative charges at pH 10.0.

Figure 4 indicates that, as the time proceeds, the streaming potential coefficient for pH 6.0 tends to decrease toward zero at the inlet position, whereas its sign is reversed from positive to negative at the outlet position about 100 min after the start of the filtration. This change is possibly due to the deposition of BSA particles onto the outer surface of the hollow fiber. The streaming potential equals zero when the positive charges of the surface are neutralized by the same number of negative charges of the particle. The positively charged pore wall is ultimately overwhelmed by the negative charges resulting from the BSA protein.

Compared to the case of pH 6.0, the increase of the absolute value of the streaming potential coefficient for pH 10.0 as the time progresses is more pronounced for the outlet position. This indicates that the negatively charged BSA particles do not deposit onto the outer surface of the negatively charged hollow fiber, due to the electrostatic repulsion at pH 10.0. Instead, they exist mainly as a suspended state above the hollow-fiber surface, which forms the concentration polarization layer. Once the cake layer is formed due to BSA deposition, it is hard to observe the increase of streaming potential because of reduction of the electrokinetic flow through the fully retentive pore. Large amounts of ionic charges existing in the concentration polarization layer provide an increasing effect of the concentration gradient. As a result, the streaming potential value becomes increased, shown in the case of pH 10.0. The absolute values of the streaming potential coefficient at an outlet of the hollow fiber are higher than those found at an inlet, since the development of axial-dependent concentration polarization of BSA particles increases as it goes to the outlet position.

Comparing the filtrate flux can be an efficient method of examining the time evolution of the streaming potential, since a trend of flux decline provides information on the concentration polarization as well as the cake layer developments during the colloid filtrations [20,21]. Figure 5 displays the variations of the filtrate flux with the filtration time. The flux decline is more considerable in the oppositely charged case of solution pH 6.0 than in the same-charged case of pH 10.0. This behavior is identical to the role of attractive electrostatic interaction resulting in a cake layer by BSA deposition onto the outer surface. As shown in Fig. 4, a reduced electrokinetic flow through the pore owing to BSA deposition leads to a decrease of the streaming potential coefficient in contrary to the same charged case.

The BSA deposition on the skin layer surface of the hollow fiber was investigated by AFM imaging with variation of surface topography at nanoscale resolution, as shown in Fig. 6. Surface roughness is related to membrane fouling. Root mean square (RMS) roughness was estimated as 5.2, 7.1, and 5.6 nm for Figs. 6a, 6b, and 6c, respectively. The roughness of the BSA-deposited hollow-fiber is greater than that for the unfouled virgin one. The BSA more uniformly covers the same charged hollow-fiber surface where a repulsive interaction exists.

As shown in Fig. 7, the streaming potential coefficient for partial retention with PM100 at pH 6.0 demonstrates a similar trend in the case of full retention, but an earlier change from positive to negative appears at about 50 min after the

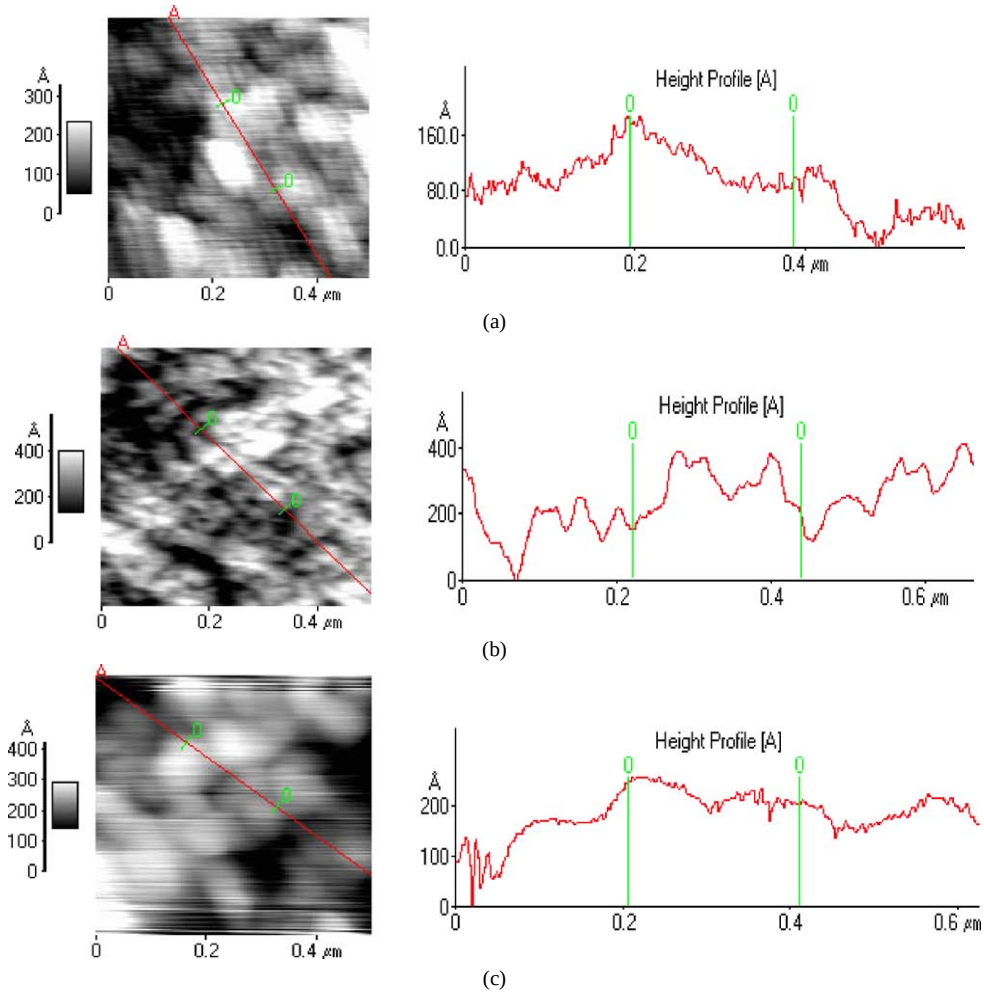

Fig. 6. AFM images of the PM10 hollow-fiber taken for the unfouled virgin fiber (a), after BSA filtration at solution pH 6 (b), and after BSA filtration at solution pH 10 (c); filtration time was 40 min.

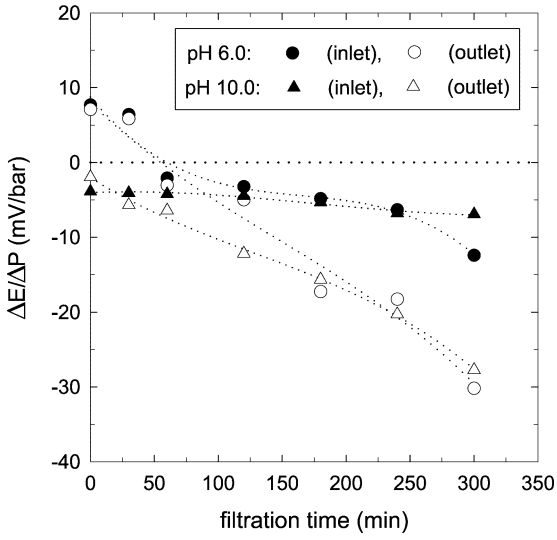

Fig. 7. Changes in the streaming potential of the partially retentive pore (PM100) during the filtration of the 90 ppm BSA solution for same-charged (pH 10.0) and oppositely charged (pH 6.0) cases, with 1.0 mM KCl concentration.

start of the filtration. Higher values of the streaming potential coefficient (ca. −30 mV/bar) are obtained at an outlet position for pH 6.0, which suggests that BSA particles adsorb on the pore wall. As the time proceeds, the absolute value of the streaming potential coefficient for pH 10.0 is increased gradually, which also may result from the partial retention property. Again, we observe that the absolute values of the streaming potential coefficient at an outlet of the hollow fiber are higher than those found at an inlet. Figure 8 shows that the flux decline of the oppositely charged case (i.e., pH 6.0) is more significant than that in the same-charged case (i.e., pH 10.0), due to the electrostatic attraction. Compared to the case of full retention provided in Fig. 5, the flux reduction decline for pH 6.0 occurs evidently at the initial stage and then the filtrate flux is almost constant.

The ratio of the streaming potential coefficient of partial retention to full retention can be estimated as provided in Fig. 9. Except for filtration time around 50 min, a streaming potential coefficient shows a larger value at partially retentive pores for the oppositely charged case of solution pH 6.0, and the increase gets larger as the filtration proceeds. In

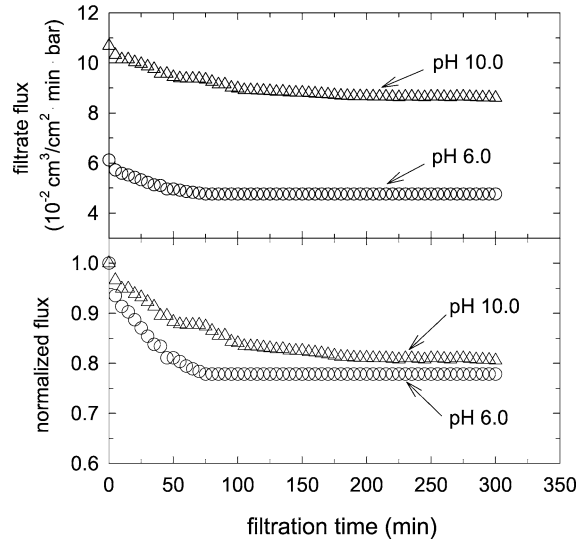

Fig. 8. Changes in the filtrate flux of the fully retentive pore (PM100) during the filtration of 90 ppm BSA solution for same-charged (pH 10.0) and oppositely charged (pH 6.0) cases, with 1.0 mM KCl concentration.

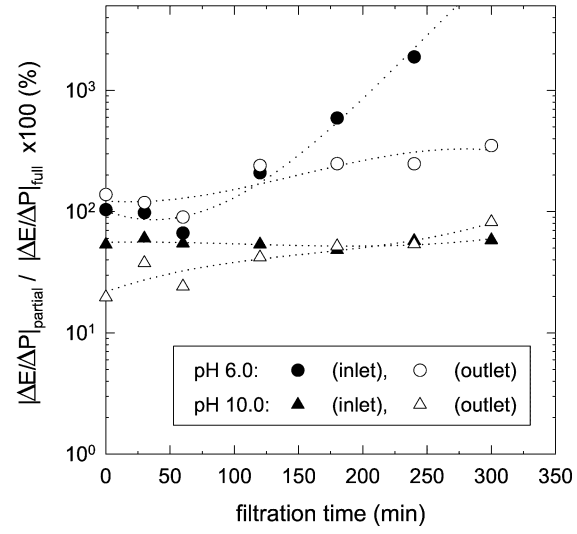

Fig. 9. The ratio of the streaming potential coefficient between partial retention and full retention versus filtration time for same-charged (pH 10.0) and oppositely charged (pH 6.0) cases.

the partially retentive pore, the BSA particles approach easily to the entrance of the oppositely charged pore and then flow through the pore channel. For the same-charged case of pH 10.0, in contrast, a streaming potential coefficient shows a lower value at the partially retentive pore. Compared to the case of pH 6.0, the BSA particles hardly flow through the channel of the same-charged pore, which results in accumulation of the BSA in the concentration polarization layer as explained above. Greater concentration gradients due to the effect of ionic charges in the concentration polarization layer incorporated with smaller pore size are expected to increase the streaming potential coefficient.

5. Conclusions

The charge characteristics of the pore walls of hollow fibers were observed by applying the apparent streaming potential based on the H–S equation, in which the surface charges of the pore wall affect both the long-range electrostatic interactions and the membrane fouling. In the fully retentive nanopore, the interaction between the protein particles and the outer surface of the hollow fiber determines the particle movement and eventually the streaming potential related to the electrokinetic flow. The streaming potential behavior in the partially retentive nanopore indicates the contribution of the additional effect of the interaction between the particles and the pore wall.

The time evolution of streaming potential coefficient for the oppositely charged case of a solution at pH 6.0 showed a change of charge condition, resulting from BSA deposition onto the outer surface of the hollow fiber. The absolute value of the streaming potential coefficient for the same-charged case of pH 10.0 was considerably increased with the filtration progress. One can say that the electrostatic repulsion allows the BSA particles to exist mainly in the concentration polarization layer instead of being deposited onto the outer surface of the hollow fiber. In any case, the time evolution of the streaming potential is closely related to the filtrate flux decline.

For the oppositely charged case, where the electrostatic attraction occurs between the positively charged pore and negatively charged BSA particles, the streaming potential gets a larger value at a partially retentive pore than at a fully retentive one. In contrast, the opposite behavior is obtained for the same-charged case, where the electrostatic repulsion is involved. It should be noted that the development of a concentration polarization layer occurring during the cross-flow filtration affects the streaming potential behavior of the hollow fiber. We also found that the streaming potential of the hollow fiber depends on the axial position, which becomes generally increasing as it goes to the downward direction.

Acknowledgment

This work was supported by the Basic Research Fund (Grant R01-2001-000-00411-0) from the Korea Science and Engineering Foundations (KOSEF).

References

[1] M. Nyström, M. Lindström, E. Matthiasson, Colloids Surf. 36 (1989) 297.
[2] C. Causserand, M. Nyström, P. Aimar, J. Membr. Sci. 88 (1994) 211.
[3] J.I. Calvo, A. Hernández, P. Pránados, F. Tejerina, J. Colloid Interface Sci. 181 (1996) 399.
[4] K.J. Kim, A.G. Fane, M. Nyström, A. Pihlajamäki, W.R. Bowen, H. Mukhtar, J. Membr. Sci. 116 (1996) 149.

[5] L. Ricq, A. Pierre, J.-C. Reggiani, J. Pagetti, A. Foissy, Colloids Surf. A Physicochem. Eng. Aspects 138 (1998) 301.
[6] D. Möckel, E. Staude, M. Dal-Cin, K. Darcovich, M. Guiver, J. Membr. Sci. 145 (1998) 211.
[7] A. Szymczyk, B. Aoubiza, P. Fievet, J. Pagetti, J. Colloid Interface Sci. 216 (1999) 285.
[8] M.C. Wilbert, S. Delagah, J. Pellegrino, J. Membr. Sci. 161 (1999) 247.
[9] I.H. Huisman, P. Prádanos, A. Hernández, J. Membr. Sci. 179 (2000) 79.
[10] M.-S. Chun, H.I. Cho, I.K. Song, Desalination 148 (2002) 363.
[11] W.B. Russel, D.A. Saville, W.R. Schowalter, Colloidal Dispersions, Cambridge Univ. Press, New York, 1989.
[12] C.L. Rice, R. Whitehead, J. Phys. Chem. 69 (1965) 4017.
[13] S. Levine, J.R. Marriott, G. Neale, N. Epstein, J. Colloid Interface Sci. 52 (1975) 136.
[14] R. Hunter, Zeta Potential in Colloid Science: Principles and Applications, Academic Press, London, 1981.
[15] A.E. Yaroshchuk, Y.P. Boiko, A.L. Makovetskiy, Langmuir 18 (2002) 5154.
[16] W.R. Bowen, P.M. Williams, Biotechnol. Bioeng. 50 (1996) 125.
[17] M. Fontyn, K. van't Riet, R.H. Bijsterbosch, Colloids Surf. 54 (1991) 331.
[18] C. Lettmann, D. Möckel, E. Staude, J. Membr. Sci. 159 (1999) 243.
[19] C. Herrero, P. Prádanos, J.I. Calvo, F. Tejerina, A. Hernández, J. Colloid Interface Sci. 187 (1997) 344.
[20] M.-S. Chun, G.-Y. Chung, J.-J. Kim, J. Membr. Sci. 193 (2001) 97.
[21] R.H. Davis, Sep. Purif. Methods 21 (1992) 75.